Biosensors and Bioelectronics 61 (2014) 88–94

Contents lists available at ScienceDirect

Biosensors and Bioelectronics

journal homepage: www.elsevier.com/locate/bios

Using protein-encapsulated gold nanoclusters as photoluminescent sensing probes for biomolecules

Karuppuchamy Selvaprakash, Yu-Chie Chen *

Department of Applied Chemistry, National Chiao Tung University, Hsinchu 300, Taiwan

ARTICLE INFO

Article history:
Received 4 February 2014
Received in revised form
11 April 2014
Accepted 29 April 2014
Available online 10 May 2014

Keywords:
Gold nanoclusters
Egg white
Ovalbumin
Adenosine-5′-triphosphate
Pyrophosphate
Photoluminescence

ABSTRACT

In this study, we generated gold nanoclusters (AuNCs) using inexpensive chicken egg white proteins (AuNCs@ew) as reagents. AuNCs@ew were generated by reacting aqueous tetrachloroauric acid with diluted chicken egg white under microwave heating (90 W) through subsequent heating cycles (5 min/cycle). Within 10 cycles, red photoluminescent AuNCs@ew with maximum emission wavelength at ~640 nm (λ_{ex}=370 nm) were obtained. The quantum yield of the as-generated AuNCs was ~6.6%. The intact and the tryptic digest of AuNCs@ew were characterized by mass spectrometry. The results showed that the AuNCs@ew were mainly derived from ovalbumin, i.e., the major protein in egg white, encapsulated AuNCs. The AuNCs@ew also has the common features found in AuNCs@protein, which is sensitive to the presence of heavy metal ions such as Cu^{2+}. The photoluminescence of the AuNCs@ew was quenched with the addition of Cu^{2+}. Furthermore, the photoluminescence of the quenched AuNCs@ew can be restored in the presence of the molecules containing phosphate functional groups because of the strong binding affinity between Cu^{2+} and phosphates. We used the AuNCs@ew-Cu^{2+} conjugates as switch-on sensing probes for the detection of phosphate containing metabolites such as adenosine-5′-triphosphate (ATP) and pyrophosphate (PPi). The results showed that the photoluminescence of the sensing probes increased as the concentration of the phosphate-containing molecules in the sample solution increased. The limits of detection achieved using the AuNCs@ew-Cu^{2+} for ATP and PPi were ~19 and ~5 μM, respectively. Additionally, we also demonstrated the feasibility of using the AuNCs@ew as the sensing probes for lectins such as concanavalin A (Con A) based on the molecular recognitions between the glycan ligands on the AuNCs@ew and glycan binding sites on Con A.

1. Introduction

Biomolecule-directed synthesis of metal nanoclusters (NCs) have attracted considerable attention because of ease of synthesis, bright photoluminescence, low toxicity, good chemical stability, and high biocompatibility (Dickerson et al., 2008). The remarkable photoluminescence property and good photo-stability of gold NCs (AuNCs) have led their applications in analytical and biochemical fields (Huang et al., 2007; Liu et al., 2013a; Guevel et al., 2011; Wu et al., 2010, and Wang et al., 2011). To date, the synthesis of different properties of AuNCs using biomolecules such as peptides (Li et al., 2012) and proteins (Lu and Chen, 2012) as reducing agents is still at the exploration stage, and more biomolecule-directed synthesis of metal NCs has yet to be discovered. Recently, protein-directed synthesis has gained increasing interest because this process provides a simple, green, and effective route for the production of metal NCs. The generation of metal NCs is usually conducted in aqueous condition, without the requirement of toxic organic solvents, thereby minimizing the possibility of environmental damage. Since Xie et al. (2009) first synthesized AuNCs using bovine serum albumin as chelating and reducing agent, different proteins (Chen et al., 2010 and Wei et al., 2010; Chan and Chen, 2012; Chen et al., 2013; Kawasaki et al., 2011) have been demonstrated to be suitable reagents for the generation of photoluminescent AuNCs. Furthermore, the generated protein-encapsulated AuNCs (AuNCs@protein) may still retain their biological activity (Chen et al., 2010 and Chan and Chen, 2012). However, one of the main concerns is the cost of proteins used in the generation of the AuNCs@protein. In previous studies (Xie et al., 2009; Chen et al., 2010; Chan and Chen, 2012; Chen et al., 2010 and Kawasaki et al., 2011), purified proteins provided by chemical companies have been generally used in the generation of AuNCs@protein; thus, the cost is quite high. If the cost of the generation of AuNCs@protein can be reduced, extended applications of using AuNCs@protein in the research of analytical chemistry and biomedicine can be expected.

The generation of AuNCs@protein is mainly counted on the composition of proteins. If proteins have sufficient numbers of the

* Corresponding author. Tel.: +886 3 5131527; fax: +886 3 5723764.
E-mail address: yuchie@mail.nctu.edu.tw (Y.-C. Chen).

http://dx.doi.org/10.1016/j.bios.2014.04.055
0956-5663/

amino acids, such as cysteine (Xie et al., 2009) and tyrosine (Xavier et al., 2010) in the protein sequences, AuNCs@protein with red photoluminescence can be readily generated by one-pot reactions. Thus, we believed that purified proteins may not be necessary for the synthesis of protein-encapsulated AuNCs. That is, in a protein mixture, only the proteins with appropriate amino acid compositions, i.e., containing a sufficient number of cysteine, can selectively react with tetrachloroauric acid to generate AuNCs@protein with red photoluminescence. Therefore, inexpensive and naturally available protein mixtures, such as protein rich eggs can be considered as one of the candidates for generating AuNCs@protein. Chicken egg white consists of ~10% proteins by weight in an egg. Ovalbumin, with the molecular weight of ~45 kDa, is the major composition in egg white proteins (~54%) (Mine, 1995) although its function in eggs is not very clear yet (Huntington and Stein, 2001). Ovalbumin contains 10 tyrosines and 6 cysteines in its protein sequence (Thompson and Fisher, 1978), leading its suitability for being used as the starting material for the generation of ovalbumin-encapsulated AuNCs (AuNCs@ova). Thus, we believed that inexpensive chicken egg white directly isolated from fresh eggs can be readily used as starting material for the generation of AuNCs@protein by one-pot reactions without purification steps. Furthermore, we expected that the AuNCs@ova may dominate the generation of AuNCs@ew.

Recently, Li et al. (2013) and Joseph and Geckeler (2014) successfully used inexpensive chicken egg white as the starting materials for generation of photoluminescent AuNCs. AuNCs@ew with red photoluminescence were obtained. Li et al. (2013) have demonstrated the application of AuNCs@ew for H_2O_2 sensing. However, the identity of the generated AuNCs@ew was not well characterized in the previous studies. The AuNCs@ew were taken as mixed protein-bound AuNCs (Li et al., 2013). If the AuNCs@ew can be well-characterized, it would be helpful to extend the applications of the AuNCs@ew in biosensing, analytical chemistry and nanomedicine. Thus, we herein characterize the identity of the AuNCs@ew by using mass spectrometry (MS) and spectroscopy. We also considered speeding up the generation of AuNCs@ew to reduce the time in the synthesis process. Thus, microwave-heating was implemented to accelerate the generation of the AuNCs@ew.

Adenosine-5′-triphosphate (ATP) and pyrophosphate (PPi) are common metabolites found in living species. The physiologic concentration of blood phosphates in healthy individuals mainly dominated by ATP is in mM level (Levi and Popovtzer, 1999). The levels of ATP and PPi in biological fluids can be used as markers for the indication of certain diseases (Bush et al., 2000, Przedborski and Vila, 2001, and Berner and Shike, 1988). Additionally, ovalbumin is a glycoprotein containing abundant glycan ligands (Harvey et al., 2000), leading the AuNCs@ew to be potential affinity-probes toward lectins that contain glycan binding sites. Thus, the feasibility of using the AuNCs@ew as the sensing probes for biomolecules including polyphosphates such as ATP and PPi and lectins such as concanavalin A was demonstrated.

2. Experimental

The details of preparation and characterization of the generated AuNCs@ew and the sensing steps for polyphosphates and Con A are provided in Supporting information.

3. Results and discussion

To accelerate the generation of AuNCs@protein, the synthesis of AuNCs was conducted in a domestic microwave oven from the one-pot reaction. The heating temperature of the domestic microwave cannot be controlled constantly. Thus, short heating cycles were employed to prevent overheating. Fig. 1A shows the fluorescence spectra (λ_{max}= 370 nm) of the reaction solution containing diluted egg white and tetrachloroauric acid acquired during the heating cycles. The heating cycles were continually conducted until the maximum fluorescence intensity at the wavelength of ~640 nm remained unchanged, indicating the end of the reaction. Fig. 1B shows the UV/vis absorption spectrum of the reaction product obtained after heated by 10 subsequent cycles. The inset shows the corresponding photographs of the reaction product taken under UV light (λ_{max}= 365 nm) (right) and room light (left). The generated AuNCs have bright and red photoluminescence under illumination of UV light, and they have pale yellow color under room light. The results indicated that egg white-encapsulated AuNCs (AuNCs@ew) with bright photoluminescence were successfully generated using the inexpensive chicken egg white as the reactant. The quantum yield (QY) of the as-prepared AuNCs@ew was estimated to be ~6.6% when using riboflavin-5′ phosphate (QY= ~26%) as a reference standard (Fig. S1). The QY of the AuNCs@ew is comparable to the AuNCs@protein reported previously (Xie et al., 2009).

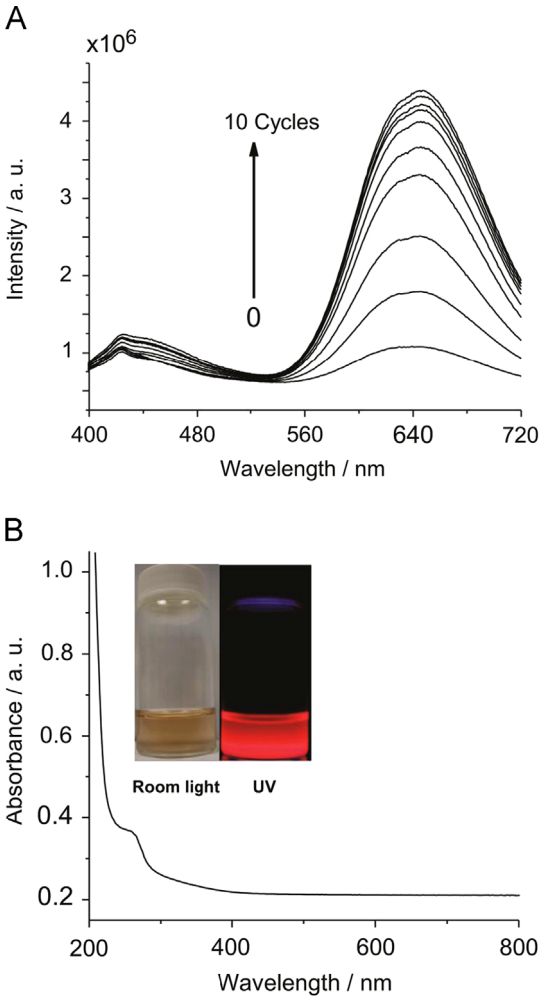

Fig. 1. (A) Fluorescence spectra (λ_{ex}= 370 nm) of the reaction solution obtained from different heating cycles in a microwave oven (90 W, 5 min cycle^{-1}). (B) UV/vis absorption spectrum of AuNCs@ew. Inset: photographs of the AuNCs@ew taken under room light and UV light (λ_{max}= 365 nm).

Fig. S2 shows the transmission electron microscopic image of AuNCs@ew. The particle size was estimated to be 2.6 ± 0.5 nm. The zeta potential of AuNCs@ew was estimated to be ~ −29 mV at pH 7, revealing that the surface charge of AuNCs@ew was negative in

neutral solution. In addition, X-ray photoelectron spectroscopy (XPS) was employed to clarify the binding between the egg white proteins and the AuNCs. The XPS results confirm the presence of Au(I) and Au(0) (Fig. S3A) and the thiol groups from cysteines in egg white proteins are involved in chelating and reducing Au precursors during the formation of AuNCs (Fig. S3B).

Fig. S4A shows the infrared (IR) spectra of egg white (red) and AuNCs@ew (black). The spectra look similar to each other, indicating that the egg white proteins were immobilized on the surface of the AuNCs. Nevertheless, the band appeared at the wavenumber of $\sim$1653 cm^{-1} (red spectrum, egg white), standing for C=O stretching and N–H bending coupled with C–N stretching (Goormaghtigh et al., 1994) shifted to 1668 cm^{-1} (black, AuNCs@ew), indicating the functional groups may have interactions between egg white proteins and the AuNCs. In addition, a very weak band appearing at the wavenumber of $\sim$2550 cm^{-1} in the IR spectrum of egg white (red) corresponding to –SH (Kemp, 1991) was absent in the IR spectrum of AuNCs@ew (black) (Fig. S4B), indicating that thiol groups were involved in the binding for the generation of the AuNCs@ew. As mentioned previously, ovalbumin is a major protein in egg white and also contains the required amino acids, such as tyrosine ($\times$ 10) and cysteine ($\times$ 6) in its protein sequence, and is thus considered as suitable reagent for the generation of AuNCs@protein. We suspected that the AuNCs@ew was mainly composed of AuNCs@ova. The IR spectrum of ovalbumin marked blue in Fig. S4A resembles that of egg white (red), implying that AuNCs@ova may dominate the generated AuNCs@ew.

To further clarify the identity of the AuNCs@ew, matrix-assisted laser desorption/ionization (MALDI) MS was used to characterize the AuNCs@ew. Fig. S5A shows the MALDI mass spectra of egg white (red) and AuNCs@ew (black). The ion peak at *m/z* $\sim$44,500 dominated the mass spectrum of the egg white (red), and its doubly charged ion peak at *m/z* $\sim$22,255 also appeared in the same mass spectrum. However, the mass spectrum of AuNCs@ew was dominated by the ion peak at *m/z* $\sim$46,500 in the mass spectrum of AuNCs@ew, and the corresponding doubly charged ion peak appeared at *m/z* $\sim$23,250. The results suggested that $\sim$10 Au atoms were encapsulated by the egg white proteins because a $\sim$2000 mass unit shift exists between the major ion peaks in the mass spectra of the egg white proteins and the AuNCs@ew. To further confirm the protein composition in AuNCs@ew, the intact AuNCs@ew was digested by trypsin followed by MALDI-MS analysis. The tryptic digestion of the AuNCs@ew was conducted based on the microwave-heating approach we proposed previously (Chen and Chen, 2007; Chan and Chen, 2012). Fig. S5B shows the resultant MALDI mass spectrum of tryptic digest of the AuNCs@ew. Through protein database search, these peaks appearing in the mass spectrum were identified as the peptides derived from chicken ovalbumin. Table S1 shows the list of the observed *m/z* and theoretical *m/z* of these peaks from the matched peptide sequences. These results indicate that AuNCs@ew were mainly composed of AuNCs@ova. As we expected, ovalbumin from complex egg white was selectively reacted with tetrachloroauric acid during the generation of the AuNCs. The results indicated that AuNCs@ova can be generated using egg white proteins from inexpensive eggs as starting materials. That is, during the reaction process, ovalbumin from complex egg white can selectively react with tetrachloroauric acid to generate AuNCs@ova with bright photoluminescence. Thus, purifying target proteins prior to the generation of the AuNCs is not necessary. Time and cost spending in the generation of AuNCs@protein can be greatly marked down using the current approach.

AuNCs@protein have been previously used as the sensing probes for metal ion detection based on the quenching effect (Xie et al., 2010). We also discovered that the photoluminescence of the as-prepared AuNCs@ew can be quenched in the presence of

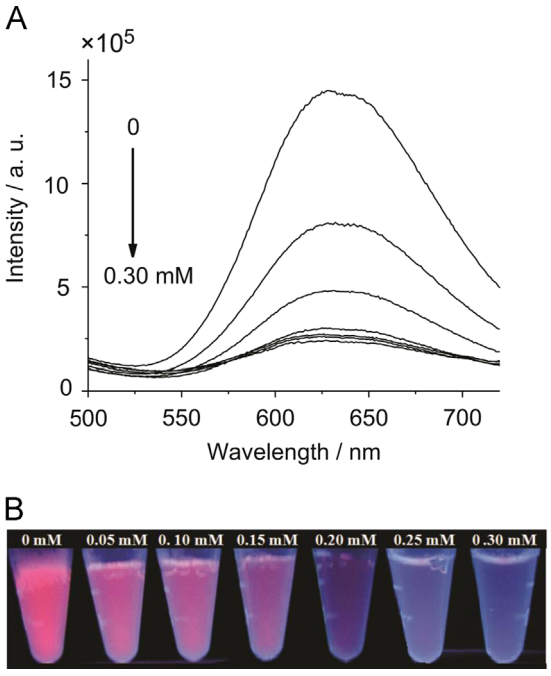

Fig. 2. (A) Fluorescence spectra obtained from the samples (0.1 mL) containing different concentrations (0, 0.05, 0.1, 0.15, 0.20, 0.25 and 0.30 mM) of Cu^{2+} with the addition of AuNCs@ew (0.1 mL, 2 mg mL^{-1}). (B) Corresponding photographs of the samples obtained from Panel A taken under illumination of UV light (λ_{max}= 365 nm). The concentrations indicated in the figure refer to the initial concentrations of Cu^{2+} prior to mixing.

Cu^{2+} and Hg^{2+}. The photoluminescence of the AuNCs@ew is not affected in the presence of Fe^{3+}/Fe^{2+}. However, considering the toxicity of Hg^{2+}, we were interested to develop sensors based on the use of the quenched AuNCs@ew-Cu^{2+}. Fig. 2A shows the fluorescence spectra of AuNCs@ew containing different concentrations of Cu^{2+}, whereas Fig. 2B shows the corresponding photographs taken under UV light (λ_{max}= 365 nm). Apparently, the fluorescence intensity of the samples gradually decreased with the increase of the concentration of Cu^{2+}. Notably, the addition of excess amount of Cu^{2+} (up to 20 mM, Fig. S6) to the aqueous AuCs@ew solution did not completely quench the fluorescence derived from the AuNCs@ew. This result shows that the remaining fluorescence of AuNCs@ew may come from Au–S binding and cannot be quenched by excess Cu^{2+}. It has been proposed that paramagnetic ions such as Cu^{2+} can quench the fluorescence of fluorophores by phosphorescence enhancement, which promotes the intersystem crossing (ISC) (Jonathan et al., 2009). Those reports also claimed that phosphorescence was too weak to be detected. That is, Cu^{2+} bound on the surface of AuNCs@ew may contribute to the loss of excited electron energy by the ISC, resulting in the quenching of the fluorescence. However, according to the XPS results shown in Fig. S3A, the oxidation number of gold on the surface of the AuNCs@ew is either 0 or +1. We were wondering how Cu^{2+} can interact directly with the positively charged core of the AuNCs@ew by considering the electrostatic force of repulsion. Thus, we postulated the other possible mechanism that may be involved in the quenching effect. According to a previous study (Wu and Jin, 2010), electron-rich functional groups (e.g., $-NH_2$, COO^-) attached on the AuNCs surface will enhance the fluorescence. Proteins are composed of amino acids that contain abundant electron-rich functional groups such as amino groups and carboxylates, while Cu^{2+} has high formation constants with amino acids (Ante and Nenad, 2011). Thus, in the presence of Cu^{2+}, it was suspected that the electron-rich ligands such as amino groups and carboxylates from the protein molecules on the

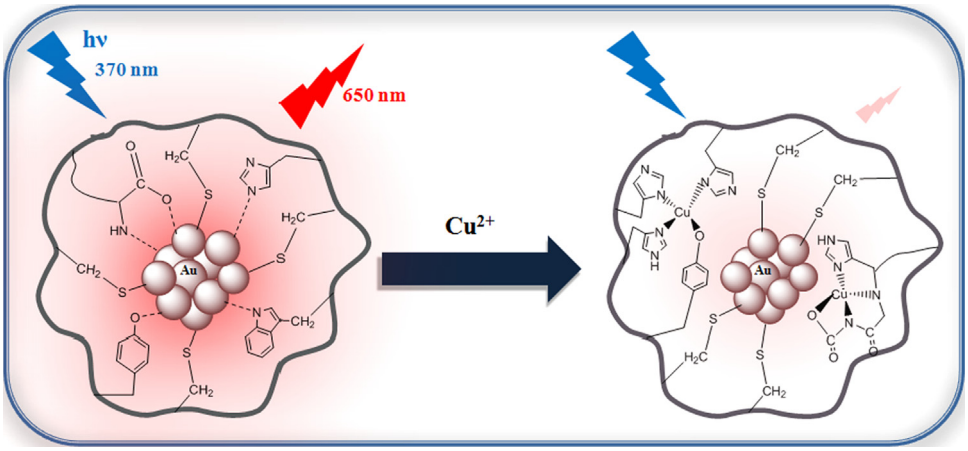

Scheme 1. Interaction of Cu^{2+} ions with amino acid moieties on the AuNCs@ew.

AuNCs@ew would chelate with Cu^{2+} and leave the surface of the AuNCs@ew (Scheme 1). As a result, the fluorescence of the AuNCs decreased because of the decrease of electron density on the surface of the AuNCs. The quenching effect was also observed when the intact AuNCs@ew was digested by trypsin digestion. When peptide residues were cut by trypsin from the surface of the AuNCs@ew, the resultant AuNCs@ew became less bright (Fig. S7). It was presumably due to fewer ligands available for binding on the core of the AuNCs@ew. A lower electron density on the surface of the AuNCs@ew resulted in lower photoluminescence. Thus, we believed that when adding sufficient amino acids to the AuNCs@ew-Cu^{2+} conjugates to compete the binding between the ligands from the protein on the AuNCs@ew and Cu^{2+}, the fluorescence of the AuNCs@ew should be able to be recovered.

To support this assumption, amino acids including glycine, arginine, alanine, lysine, proline, and aspartic acid were added to the quenched AuNCs@ew-Cu^{2+} to investigate whether the fluorescence of the AuNCs@ew can be restored or not. Figs. S8A to S8F show the resultant fluorescence spectra of AuNCs@ew-Cu^{2+} with addition of glycine, arginine, alanine, lysine, proline and aspartic acid, respectively, with different concentrations. Apparently, the fluorescence intensity of AuNCs@ew-Cu^{2+} was recovered gradually with the increase of the concentration of amino acids. The results showed that the quenching effect is reversible. The results also indicated that the additional amino acids can remove Cu^{2+} from the AuNCs@ew-Cu^{2+} owing to their strong binding interactions. Therefore, electron-rich functional groups from proteins on the AuNCs@ew could re-attach to the surface of the AuNCs@ew. The increased electron density on the surface of the AuNCs@ew led the AuNCs@ew to re-gain their fluorescence as the mechanism is proposed in Scheme 1.

We further designed the AuNCs@ew-Cu^{2+} as sensing probes for phosphate-containing molecules. Phosphates are good chelating ligands for Cu^{2+}, and the formation constants of ATP, PPi, and Cu^{2+} are log K_1=6.1 and 6.7 (Furia, 1972), respectively. Thus, we believed that the quenched AuNCs@ew-Cu^{2+} can be used as "turned-on" sensing probes for the detection of phosphate-containing molecules such as ATP and PPi. To examine the feasibility of using the AuNCs@ew-Cu^{2+} as the switch-on sensing probes for phosphate containing molecules, aqueous samples spiked with different concentrations of PPi were used as the model samples. After adding the AuNCs@ew-Cu^{2+} sensing solution, the fluorescence intensity of the mixture gradually increased as the concentration of PPi increased (Fig. 3A). Fig. 3B shows the corresponding photographs of the resultant samples under UV light illumination. The photoluminescence became brighter as the concentration of PPi increased. Fig. 3C shows the corresponding plot obtained from the fluorescence change at the emission

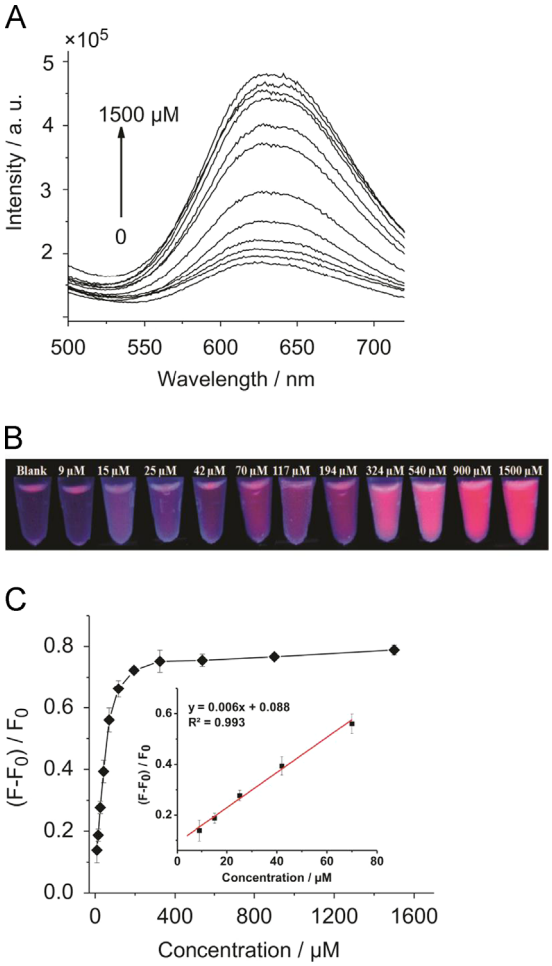

Fig. 3. (A) Representative fluorescence spectra of the supernatants obtained by vortex-mixing the samples containing different concentrations (0–1500 μM) of PPi (50 μL) with the sensing solution (150 μL) for 20 min, followed by centrifugation at 10,000 rpm for 15 min. (B) Corresponding photographs of the samples obtained from Panel A taken under a UV light (λ_{max}= 365 nm). (C) Concentration–response curve derived from Panel A. Each data point was obtained from three replicates. Inset: the calibration curve was obtained based on the linear range from 9 to 70 μM. *F* stands for the fluorescence intensity at the wavelength of 640 nm (λ_{ex}= 370 nm) of the resulting supernatant, while F_0 represents the fluorescence intensity of the blank control sensing solution.

wavelength at ~640 nm (λ_{ex}= 370 nm) versus the concentration of PPi. The linear regression coefficient (R^2=0.993) between the concentration of 0 μM to 70 μM was obtained. The limit of

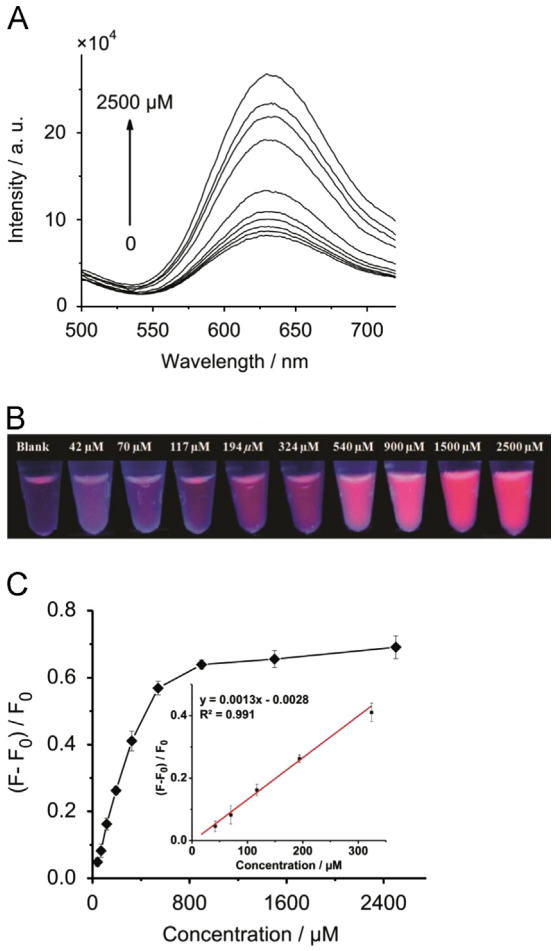

Fig. 4. (A) Representative fluorescence spectra of the supernatants obtained by vortex-mixing the samples containing different concentrations (0–2500 μM) of ATP (50 μL) with the sensing solution (150 μL) for 20 min followed by centrifugation at 10,000 rpm for 15 min. (B) Corresponding photographs of the resultant samples obtained from Panel A. The photographs were taken under illumination of UV light (λ_{max}=365 nm). (C) Concentration–response curve derived from Panel A. Each data point was obtained from three replicates. Inset: the calibration curve was obtained based on the linear range from 42 to 324 μM. *F* stands for the fluorescence intensity at the wavelength of 640 nm (λ_{ex}= 370 nm) of the resulting supernatant, while F_0 represents the fluorescence intensity of the blank control sensing solution.

detection (LOD) was estimated to be ~5 μM based on 3SD/S, in which SD is the standard error of the intercept and S is the slope of the calibration curve.

In addition, we also used ATP as the model sample for investigating the switch-on sensing capability of the AuNCs@ew-Cu^{2+}. Fig. 4A shows the fluorescence spectra obtained from the samples containing different concentrations of ATP with the addition of AuNCs@ew-Cu^{2+} as the sensing solution. The fluorescence intensity of the samples increased with the increase in the concentration of ATP in the sample solution. Furthermore, it is apparent that the sample solution became brighter as the concentration of ATP in the sample solution increased (Fig. 4B). Fig. 4C shows that the plot of the fluorescence change at the emission wavelength of ~640 nm (λ_{ex}= 370 nm) versus the concentration of ATP. A good linear regression coefficient was also obtained (R^2= 0.991), indicating the possibility of using the current approach for quantitative analysis. The LOD was estimated to be ~19 μM based on 3SD/S. The results indicate that the AuNCs@ew-Cu^{2+} complexes can be used as suitable sensing probes for PPi and ATP. Compared with the LOD obtained using AuNCs (Li et al., 2012) and quantum dots (Liu et al., 2013b) as the sensing probes for PPi and ATP, our approach is comparable.

The applicability of the proposed "off-to-on" properties of AuNCs@ew-Cu^{2+} for the assay of human serum samples was further evaluated. Although our sensors are sensitive to both PPi and ATP, the concentration of PPi in serum is much lower than ATP (Sakamoto et al., 2009). Notably, the photoluminescence of the AuNCs@ew-Cu^{2+} was not affected much in the presence of monophosphate with the concentration up to 2.5 mM (Fig. S9). Thus, in a serum sample, the sensing response toward the sensing probes is mainly contributed by ATP. To estimate the level of ATP from human serum samples, the standard addition method by spiking different concentrations of ATP to diluted human serum samples was conducted. Fig. S10A shows the representative fluorescence spectra obtained from the supernatant. The fluorescence intensity was apparently enhanced with the increase of ATP in the human serum samples. Fig. S10B shows the corresponding calibration curve obtained by plotting the intensity at the emission wavelength of 640 nm (λ_{ex}= 370 nm) versus the concentration of ATP spiked in the serum samples. On the basis of this plot, we estimated ~4.1 mM of ATP present in the serum sample, while ~3.3 mM of ATP was estimated in the same serum sample by using commercial ATP bioluminescent assay kit (Fig. S11). The results show that the ATP level obtained from our sensing method was close to that obtained from bioluminescent assay, and also suggest that our current approach can be used to roughly estimate the concentration of ATP in serum samples.

Ovalbumin is a glycoprotein and contains abundant glycan ligands. Since the AuNCs@ew are mainly dominated by the AuNCs@ova, we further used the AuNCs@ew as the sensing probes for lectins such as Con A, which contain glycan binding sites. Con A has been demonstrated as a potential anti-cancer drug (Shi et al., 2014). Thus, it is vital to develop sensing methods that can monitor the level of Con A in serum samples. The selectivity of the AuNCs@ew toward different proteins was investigated. AuNCs@ew and protein solution were vortex-mixed for 2 h followed by centrifugation at 10,000 rpm for 1 h. Apparently, only the vial containing Con A showed obvious precipitates (Fig. 5A), resulting from the conjugates of AuNCs@ew-Con A. No precipitation was observed in the rest of the sample vials. The results indicated that our AuNCs@ew have selectivity toward Con A, leading the formation of the conjugates of AuNCs@ew-Con A. We further examined the possibility of using this approach for quantitative analysis. Fig. 5B shows the representative fluorescence spectra of the supernatant obtained by vortex-mixing the AuNCs@ew with different concentrations of Con A, while Fig. 5C shows the corresponding plot (y= 0.039 x−0.078, R^2= 0.983; linear range: 0–15 μM) obtained by plotting the intensity at the emission wavelength at 640 nm (λ_{ex}=370 nm) versus the concentration of Con A. The LOD was estimated to be ~600 nM based on 3SD/S. To examine the interference contributed from complex matrix, we prepared simulated sample by spiking Con A (3.7 μM) to a 50-fold diluted serum sample (pH 7.5). Fig. S12 shows the resultant fluorescence spectra of the supernatant samples obtained from vortex-mixing the AuNCs@ew with the diluted serum samples with Con A (blue) and without Con A (black). On the basis of the plot in Fig. 5C, the concentration of Con A was estimated to be ~3.9 μM. The experimental value was ~5% off from the true one. The results showed that it is potentially possible to use this cost-effective AuNCs@ew as the sensing probes for lectins from complex samples. However, standard addition method should be carried out if real samples are examined.

4. Conclusion

A cost effective and straightforward approach for generation of the photoluminescent AuNCs sensors for phosphate-

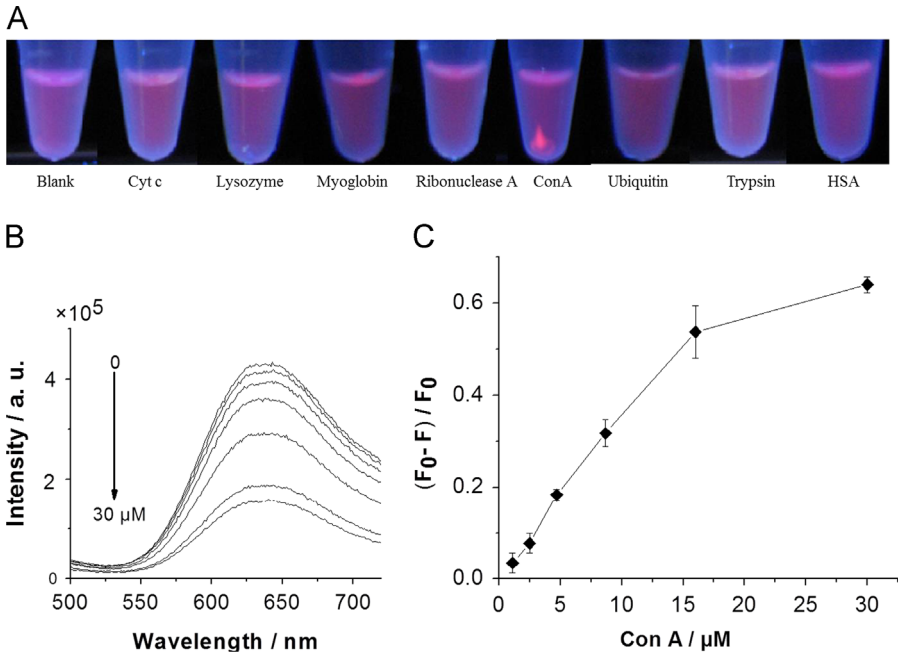

Fig. 5. (A) Photographs obtained after mixing individual protein samples including cytochrome c (Cyt c), lysozyme, myoglobin, ribonuclease A, Con A, ubiquitin, tryspin, and human serum albumin (HSA) with the AuNCs@ew for 2 h followed by centrifugation at 10,000 rpm for 1 h. (B) Representative fluorescence spectra of the supernatants obtained by vortex-mixing the samples containing different concentrations of Con A (30 μL) with the AuNCs@ew (0.25 mg/mL, 30 μL) for 2 h followed by centrifugation at 10,000 rpm for 1 h. (C) Plot derived from Panel B. All the samples were prepared in HEPES buffer (pH 7.5).

containing molecules such as ATP and PPi has been demonstrated in this work. By simply reacting inexpensive egg white with tetrachloroauric acid at a basic condition under microwave-heating, the AuNCs@ew can be readily generated. Although the cost for the generation of the AuNCs@ew is relatively low compared with those generated from purified proteins, the sensing capability of the AuNCs@ew-Cu^{2+} toward ATP and PPi is comparable to those generated from expensive and purified proteins. Additionally, we also demonstrated the AuNCs@ew were mainly dominated by the AuNCs@ova through careful characterization. Since ovalbumin is a glycoprotein and contains abundant glycan ligands, the feasibility of using the AuNCs@ew directly as the sensing probes for Con A, which contains glycan binding sites, has been successfully demonstrated in this study. We believe that the glycan-ligand rich AuNCs@ew can be further developed to be sensing probes for other targets containing glycan-binding sites. Furthermore, the advantages of low cost and ease-of-synthesis would potentially lead the protein-encapsulated AuNCs to be more popular in the research of biochemical/chemical sensing. Furthermore, the cost-down approach leads the promising of further exploration of other naturally available proteins as the starting materials for the generation of the AuNCs@protein. Thus, we are quite optimistic about the further development and applications of this approach.

Acknowledgments

We thank the Ministry of Science and Technology of Taiwan (NSC 102–2113-M-009–019-MY3 and NSC 102–2627-M-009-002) for financial support of this work. We also thank C.-Y. Wu for her assistance in obtaining TEM images and Prof. S.-B. Wu for loaning us the spectrofluorophotometer. KS thanks NCTU for the NCTU International Students Scholarship.

Appendix A. Supporting information

Supplementary data associated with this article can be found in the online version at http://dx.doi.org/10.1016/j.bios.2014.04.055.

References

Ante, M., Nenad, R., 2011. Chin. J. Chem. 29, 1800–1804.
Berner, Y.N., Shike, M., 1988. Annu. Rev. Nutr. 8, 121–148.
Bush, K.T., Keller, S.H., Nigam, N.K., 2000. J. Clin. Invest. 106, 621–626.
Chan, P.-H., Chen, Y.-C., 2012. Anal. Chem. 84, 8952–8956.
Chen, W.-Y., Chen, Y.-C., 2007. Anal. Chem. 79, 2394–2401.
Chen, W.-Y., Lin, J.-Y., Chen, W.-J., Lo, L., Diau, E.W.G., Chen, Y.-C., 2010. Nanomedicine 5, 755–764.
Chen, Y., Wang, Y., Wang, C., Li, W., Zhou, H., Jiao, H., Lin, Q., Yu, H., 2013. J. Colloid. Interface Sci. 396, 63–68.
Dickerson, M.B., Sandhage, K.H., Naik, R.R., 2008. Chem. Rev. 108, 4935–4978.
Furia, T.E., 1972. CRC Handbook of Food Additives. CRC press, Ohio, USA.
Goormaghtigh, G., Cabiaux, V.J., Ruysschaert, J.M., 1994. Subcell. Biochem. 23, 329–362.
Guevel, X.L., Daum, N., Schneider, M., 2011. Nanotechnology 22, 275103.
Harvey, D.J., Wing, D.R., Küster, B., Wilson, I.B., 2000. J. Am. Soc. Mass Spectrom. 11, 564–571.
Huang, C.C., Yang, Z.S., Lee, K.H., Chang, H.T., 2007. Angew. Chem. Int. Ed. 46, 6824–6828.
Huntington, J.A., Stein, P.E., 2001. J. Chromatogr. B 756, 189–198.
Jonathan, J.B., Clayton, G., Andrew, R.B., 2009. J. Phys. Chem. C 113, 4270–4276.
Joseph, D., Geckeler, K.E., 2014. Colloids Surf. B 115, 46–50.
Kawasaki, H., Hamaguchi, K., Osaka, I., Arakawa, R., 2011. Adv. Funct. Mater. 21, 3508–3515.
Kemp, W., 1991. Organic Spectroscopy. Palgrave Macmillan Limited, New York.
Levi, M., Popovtzer, M., 1999. Disorders of phosphate balance, Atlas of Diseases of the Kidney. Current Medicine, Inc, Philadelphia, PA.
Li, M., Yang, D.-P., Wang, X., Lu, J., Cui, D., 2013. Nano Res. Lett. 8, 182.
Li, P.-H., Lin, J.-Y., Chen, C.-T., Ciou, W.-R., Chan, P.-H., Luo, L., Hsu, H.-Y., Diau, E.W.G., Chen, Y.-C., 2012. Anal. Chem. 84, 5484–5488.
Liu, J.M., Chen, J.T., Yan, X.P., 2013a. Anal. Chem. 85, 3238–3245.
Liu, J., Zhang, X.L., Cong, Z.X., Chen, Z.T., Yang, H.H., Chen, G.N., 2013b. Nanoscale 5, 1810–1815.
Lu, Y., Chen, W., 2012. Chem. Soc. Rev. 41, 3594–3623.
Mine, Y., 1995. Trends Food Sci. Technol. 7, 225–232.
Przedborski, S., Vila, M., 2001. Clin. Neurosci. Res. 1, 407–418.
Sakamoto, T., Ojida, A., Hamachi, I., 2009. Chem. Commun., 141–152.
Shi, Z., Chen, J., Li, C.-Y., An, N., Wang, Z.-J., Yang, S.-L., Huang, K.-F., Bao, J.-K., 2014. Acta Pharmaco. Sin. 35, 248–256.

Thompson, E.O., Fisher, W.K., 1978. Aust. J. Biol. Sci. 31, 433–442.
Wang, H.H., Lin, C.A., Lee, C.H., Lin, Y.C., Tseng, Y.M., Hsieh, C.L., Chen, C.H., Tsai, C.H., Hsieh, C.T., Shen, J.L., Chan, W.H., Chang, W.H., Yeh, H.I., 2011. ACS Nano 5, 4337–4344.
Wei, H., Wang, Z., Yang, L., Tian, S., Hou, C., Lu, Y., 2010. Analyst 135, 1406–1410.
Wu, X., He, X., Wang, K., Xie, C., Zhou, B., Qing, Z., 2010. Nanoscale 2, 2244–2249.
Wu, Z., Jin, R., 2010. Nano Lett. 10, 2568–2573.
Xavier, P.L., Chaudhari, K., Verma, P.K., Pal, S.K., Pradeep, T., 2010. Nanoscale 2, 2769–2776.
Xie, J., Zheng, Y., Ying, J.Y., 2009. J. Am. Chem. Soc. 131, 888–889.
Xie, J., Zheng, Y., Ying, J.Y., 2010. Chem. Commun. 46, 961–963.